High Performance Reversible Furan-Maleimide Resins Based on Furfuryl Glycidyl Ether and Bismaleimides

Jiawen Wang , Jixian Li , Jun Zhang , Shuyue Liu , Liqiang Wan , Zuozhen Liu , Farong Huang *

Posted Date: 30 June 2023

doi: 10.20944/preprints202306.2118.v1

Keywords: Diels-Alder reaction; furan-maleimide resin; thermally reversible cross-linking resins; high performance resin

Article

High Performance Reversible Furan-Maleimide Resins Based on Furfuryl Glycidyl Ether and Bismaleimides

Jiawen Wang [1], Jixian Li [1], Jun Zhang [1], Shuyue Liu [1], Liqiang Wan [1], Zuozhen Liu [1,2] and Farong Huang [1,*]

[1] Key Laboratory for Specially Functional Materials and Related Technology of Ministry of Education, School of Materials Science and Engineering, East China University of Science and Technology, Shanghai 200237, China

[2] Huachang Polymers Co., Ltd. East China University of Science and Technology, Shanghai 200241, China

* Correspondence: fhuanglab@ecust.edu.cn

Abstract: Two reversible furan-maleimide resins, in which there are rigid -Ph-CH_2-Ph- structure and flexible -$(CH_2)_6$- structures in bismaleimides, were synthesized from furfuryl glycidyl ethers (FGE), 4,4′-diaminodiphenyl ether (ODA), *N,N*'-4,4'-diphenylmethane-bismaleimide (DBMI) and *N,N*'-hexamethylene-bismaleimide (HBMI). The structures of the resins were confirmed by Fourier transform infrared analysis, and the thermoreversibility was evidenced by differential scanning calorimetry (DSC) analysis as well as sol-gel transformation process. Mechanical properties and recyclability of the resins were preliminarily evaluated by the flexural test. The results show the Diels-Alder (DA) reaction occurs at about 90°C and reversible DA reaction does at 130-140°C for the furan-maleimide resin. Thermally reversible furan-maleimide resins have high mechanical properties. The flexural strength of cured FGE-ODA-HBMI resin arrives at 141 MPa. The resins have a repair efficiency of over 75%. After being hot-pressed for three times, two resins display higher flexural strength than 80 MPa.

Keywords: Diels-Alder reaction; furan-maleimide resin; thermally reversible cross-linking resins; high performance resin

1. Introduction

Thermosetting resins are a class of highly cross-linking polymers that are often mechanically strong and hard [1]. Therefore, thermosetting resins are indispensable in the fields of composite materials, structural adhesives, electronic packaging materials, and protective coatings [2]. Thermosetting resins form three-dimensional networks connected to each other by covalent bonds after curing. Covalent bonds are usually strong but irreversible, making thermosetting resins difficult to be reprocessed. This runs counter to the goal of achieving a circular economy [3]. Fortunately, introducing dynamic reversible bonds allows for the recycle of strong thermosetting resins [1]. Moreover, dynamic reversible reactions produce no additional products and do not demand any other reactants, meaning they are carbon-economical. Nowadays, dynamic covalent bonds are widely used to prepare dynamically reversible cross-linked resins. The reactions that generate dynamic covalent bonds include Diels-Alder (DA) reaction [4,5], disulfide bond exchange reaction [6,7], interesterification reaction [8,9], transamidation reaction [10], imine and acylhydrazone bond exchange reaction [11,12], siloxane equilibrium reaction [13], alkyl transfer reaction [14], and olefin metathesis reaction [15].

The DA reaction is ideal for preparing thermally stimulated repair polymeric materials due to its good thermal reversibility, high yield, few side reactions, and mild reaction conditions. Most studies have focused on the DA reaction between furan (diene) and maleimide (dienophile) due to the high reactivity exhibited by the imide group [16]. The furan ring shows a distinct diene character rather than an aromatic ring, which means that its chemical behavior is more similar to

 doi:10.20944/preprints202306.2118.v1

cyclopentadiene than benzene [17]. Bismaleimide (BMI) resins are bifunctional thermosetting resins with maleimide as the reactive end group [18]. BMI resins have high mechanical properties, and dimensional stability. However, they are not recycled due to the high crosslinking structures after curing [19]. Furan-maleimide resins based on the DA reaction undergo a [4+2] reaction between furan rings and maleimide groups at lower temperatures. The reversible-DA (r-DA) reaction occurs above 120°C so that furan-maleimide resins are depolymerized into furan and maleimide [20]. Fan et al. [21] prepared a series of recyclable polymers via a Diels-Alder reaction between furan-functionalized poly(hydroxyamino ether) and 1,5-bis(maleimide)-2-methylpentane. In their work, the crosslink density of the recyclable network was adjusted by varying the content of the flexible -(CH_2CH_2O)- structure. They found that with the rise in the content of the flexible structure, the glass transition temperature decreased while the r-DA reaction temperature increased. Currently, most of the furan-maleimide resins reported in literatures have flexural strengths below 50 MPa [22,23]. The introduction of flexible chains is a common method to improve the mechanical properties of resins [24]. Ma et al. increased the impact strength by up to 100% by introducing the poly(ethylene glycol) structure into polytriazole resins [25].

In this paper, two reversible furan-maleimide resins with either rigid -Ph-CH_2-Ph- structure or flexible -(CH_2)$_6$- structure in the bismaleimide units were prepared by one-pot synthesis using furfuryl glycidyl ether (FGE), 4,4′-diaminodiphenyl ether (ODA), *N,N*'-4,4'-diphenylmethane-bismaleimide (DBMI) and *N,N*'-hexamethylene-bismaleimide (HBMI) as the raw materials. The curing behaviors, thermal properties, mechanical properties, and reversible properties of the resins were investigated, and meanwhile the effect of flexible structures on the properties was discussed.

2. Materials and Methods

2.1. Materials

Furfuryl alcohol, tetrabutylammonium bromide, epichlorohydrin, maleic anhydride, sodium hydroxide (NaOH), anhydrous sodium sulphate (Na_2SO_4), ethyl acetate, 1,6-hexanediamine, *N,N*'-dimethylformamide (DMF), sodium acetate (AcONa), acetic anhydride ($(Ac)_2O$), triethylamine (TEA), sodium bicarbonate ($NaHCO_3$), petroleum ether, 4,4'-oxydianiline (ODA), and *N,N*'-4,4'-diphenylmethane-bismaleimide (DBMI) were obtained from Shanghai Titan Technology Co. All reagents were in analytical reagent grade.

2.2. Instruments and measurements

Fourier transform infrared (FT-IR) spectrum was measured with a Nicolet iS10 infrared spectrometer (Thermo Scientific Corporation, USA). The scanning range was 400-4000 cm^{-1} with the resolution of 4 cm^{-1} and the scanning times of 32. The proton nuclear magnetic resonance (^{1}H-NMR) spectrum was carried out on an AVANCE Ⅲ 400 spectrometer (Bruker, Switzerland) operating at 400 MHz with deuterated chloroform ($CDCl_3$) as the solvent and tetramethylsilane (TMS) as the internal standard. Melting point (T_m) was measured with a X4 melting apparatus (Shanghai Analytic Instrument Factory, China). Electron impact mass spectrometry (EI-MS) spectrum was performed using the GCT Premier EI-TOF mass spectrometer (Waters, USA) with m/z range of 10-1500 Da. Differential scanning calorimetry (DSC) analysis was carried out with a TA Instruments Q2000 analyzer (TA, USA) by setting a ramp from 40°C to 300°C with a heating rate of 10°C/min, and a N_2 flow of 50 mL/min. Thermogravimetric analysis (TGA) was carried out on a TGA/DSC 1LF analyzer (METTLER TOLEDO, Switzerland) in N_2 with a gas flow rate of 60 mL/min and a heating rate of 10°C/min. The flexural properties were tested according to GB/T 2567-2021 on an electronic universal testing machine (SANS CMT 4204, China). The three-point flexural model was used for the test, and the test loading speed was 2 mm/min. The size of the sample for the flexural test was 80×15×4 mm^3.

The content of soluble components of the resins in acetone with different structures was measured with Soxhlet extractor. Resins with mass m_0 were put in extractor, and continuous extraction at reflux temperature of acetone for 24 h was conducted. Then the resins after extraction were taken out

Preprints (www.preprints.org) | NOT PEER-REVIEWED | Posted: 30 June 2023 doi:10.20944/preprints202306.2118.v1

and dried under vacuum. Afterwards, the resins were weighed and recorded as m_1. The content of soluble components (S) in the resins was calculated according to Equation (1).

$$S=\frac{m_0-m_1}{m_0}\times 100\% \quad (1)$$

The reversibility of the resins was verified by hot-pressing process. The resins were first cut into small scraps, and then the scraps were pressed in a flat vulcanizing machine at 140°C under the pressure of 3 MPa for 30 min. Afterwards, the pressed scraps were continually placed at 90°C for 24 h.

2.3. Synthesis of furfuryl glycidyl ether (FGE)

The synthesis of FGE was shown in Scheme 1. Furfuryl alcohol (FAL, 9.82 g, 0.100 mol), tetrabutylammonium bromide (TBAB, 0.450 g, 14.0 mmol) was added to a three-necked flask equipped with a reflux condenser, a thermometer and a mechanical stirrer. Epichlorohydrin (ECH 10.2 g, 0.110 mol) was dropped into the flask under inert gas protection and the reaction mixture was stirred vigorously at room temperature for 4 h. Then the mixture was cooled to 10°C with an ice bath and 50*wt*% NaOH aqueous solution (20 mL) was slowly added into the flask. After the reaction mixture was stirred for 2 h at ambient temperature, 30 mL deionized water was added. The product was extracted with 10 mL ethyl acetate and the organic phase was separated in a separator. The extraction was conducted three times. The organic extracted product was collected and washed for three times with deionized water. The organic phase was separated out, dried with anhydrous Na_2SO_4 and filtrated to give a transparent solution. Then the solvent in solution was removed under reduced pressure to get an orange-yellow liquid. And the liquid was further purified by column chromatography with a mixed solvent of acetate/petroleum = 1/1 to obtain a light yellow liquid product (FGE, yield 78%) [16,26]. ^{1}H-NMR (400 MHz, $CDCl_3$) δ: 7.44-7.39 (t, 1H, -O-C**H**=CH-), 6.38-6.31 (d, 2H, =C**H**-C**H**=), 4.53 (q, 2H, C-C**H$_2$**-O), 3.80-3.40 (q, 2H, -O-C**H$_2$**-CH), 3.16 (m, 1H, 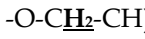), 2.80-2.61 (t, 2H,). FT-IR (KBr, cm^{-1}): 3146, 3125(=C-H, υ), 3062 (-C-H on the oxirane ring, υ), 1504 (-C=C-, υ), 1257, 850 (C-O-C on the oxirane ring, υ), 1217, 1084 (CH_2-O-CH_2, υ), 1150 (C-O-C on the furan ring, υ), 1008 (C-O-C on the furan ring, δ), 918 (C-O-C on the oxirane ring, δ), 751 (single-substituted furan ring, δ). EI-MS(m/z): 154 $[M]^+$, 97 [M- 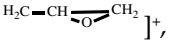]$^+$, 81 [M-]$^+$ (Figure S1).

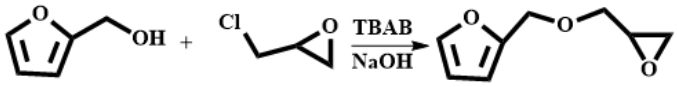

Scheme 1. Synthetic route of FGE.

2.4. Synthesis of N, N'-hexamethylene-bismaleimide (HBMI)

The synthesis of HBMI was shown in Scheme 2. 1,6-Hexanediamine (HDA, 11.6 g, 0.100 mol) and DMF (100 mL) were added to a four-necked flask equipped with a reflux condenser, a thermometer and a mechanical stirrer. Maleic anhydride (21.6 g, 0.220 mol) dissolved in DMF (100 mL) was dropped into the flask and the mixture was stirred at 90°C for 3 h. At the end of the reaction, the mixture was cooled to 60°C, after which AcONa (2.00 g, 0.0244 mol) was added and a mixture of $(Ac)_2O$ (100 mL) and TEA (20 mL) was dropped into the flask. Then the mixture was heated at 90°C for another 3 h. The reaction solution was washed with ice water. The solid was separated and washed with saturated $NaHCO_3$ followed by washing with deionized water several times to obtain a yellow powder. Finally, the powder was dried in a vacuum oven at 100°C for 12 h. A light yellow powder was obtained as the final product, *N,N'*-hexamethylene-bismaleimide (HBMI, yield 56%, T_m 137-138°C) [27]. ^{1}H-NMR (400 MHz, $CDCl_3$) δ: 6.60 (s, 4H, **H**C=C**H**), 3.39 (t, 4H, -NC**H$_2$**-), 1.56-1.34 (m, 4H, -NCH_2C**H$_2$**-), 1.34-1.09 (m, 4H, -NCH_2CH_2C**H$_2$**). FT-IR (KBr, cm^{-1}): 3107 (=C-H, υ), 2942 (-CH_2-, υ), 1690 (C=O, υ), 1587, 1453 (C=C, υ), 1227 (C-N, υ), 698 (=C-H, δ). EI-MS(m/z): 276 $[M]^+$, 110 [M- 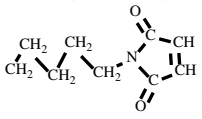]$^+$, 82 [M- 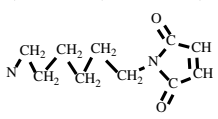]$^+$ (Figure S2).

Preprints (www.preprints.org) | NOT PEER-REVIEWED | Posted: 30 June 2023 doi:10.20944/preprints202306.2118.v1

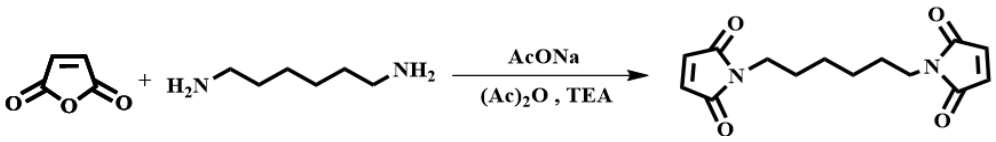

Scheme 2. Synthetic route of HBMI.

2.5. Synthesis of cured FGE-ODA-BMI resins

The synthesis of two FGE-ODA-BMI resins, namely FGE-ODA-DBMI resin and FGE-ODA-HBMI resin, is shown in Scheme 3. The synthesis of FGE-ODA-DBMI is taken as an example to demonstrate the synthesis details. FGE (5.15 g, 3.30 mmol), *N,N*'-4,4'-diphenylmethane-bismaleimide (DBMI 5.98 g, 16.7 mmol), and DMF (5 mL) were added to a 100 mL three-necked flask equipped with a stirrer, a thermometer and a condenser. After that, the temperature of the mixture was slowly raised to 55°C under stirring until the mixture became transparent. Then 4,4′-diaminodiphenyl ether (ODA, 1.65 g, 8.25 mmol) was added into the flask. The mixture was stirred well. A certain amount of the mixture was put into a preheated mold covering a release agent in a 125°C vacuum oven for 30 min to remove residual solvents. Then a reddish brown liquid was formed at 125°C (FGE-ODA-DBMI resin) [28], after the resins were heated at 110°C for 12 h and at 90°C for 24 h, a reddish-brown cured FGE-ODA-DBMI resin and cured FGE-ODA-HBMI resin were obtained.

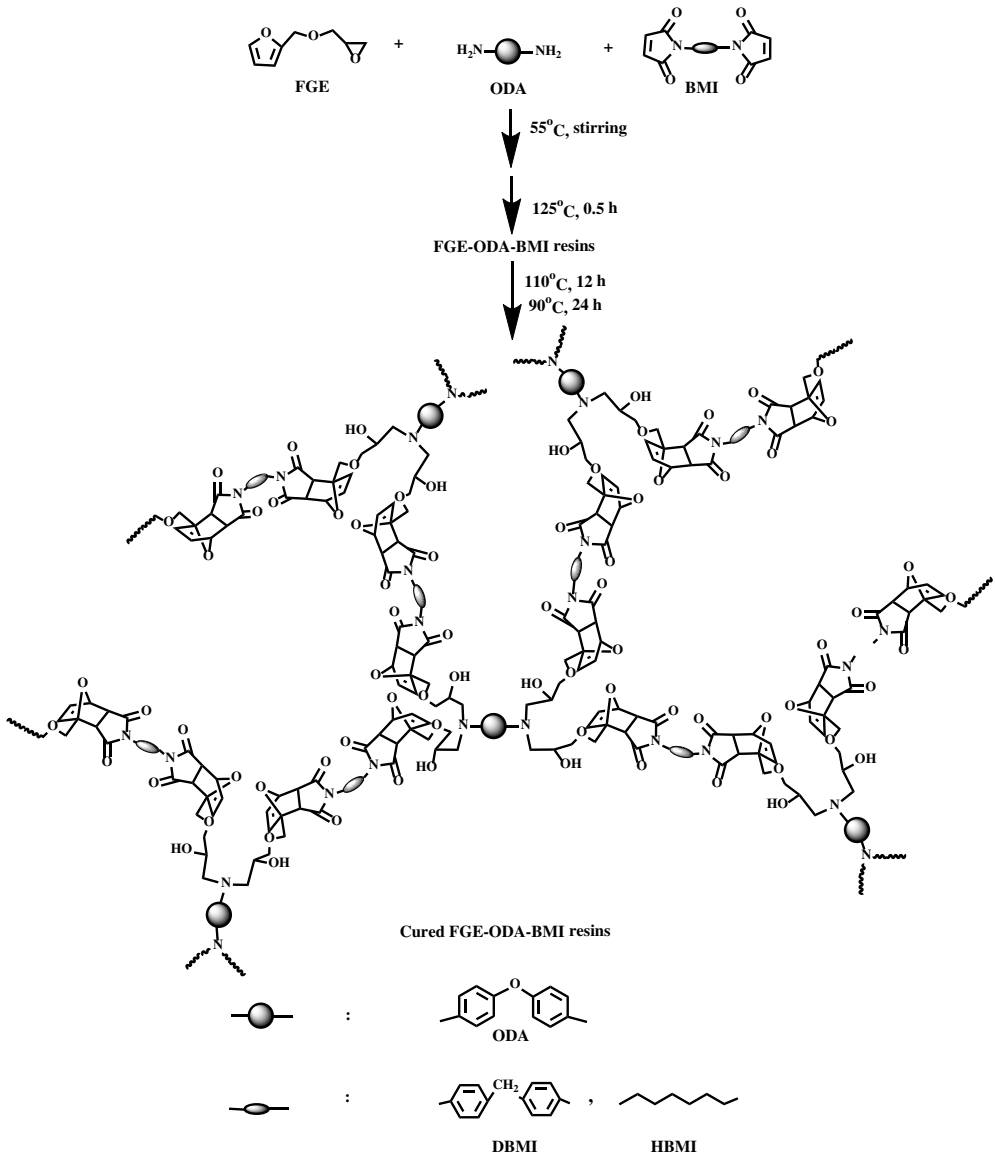

Scheme 3. Synthetic route of cured FGE-ODA-BMI resins.

Preprints (www.preprints.org) | NOT PEER-REVIEWED | Posted: 30 June 2023 doi:10.20944/preprints202306.2118.v1

3. Results

3.1. Curing procedures and structural characterization of FGE-ODA-BMI resins

The reactions between FGE and DBMI, FGE and ODA, DBMI and ODA, and among DBMI, FGE and ODA are investigated by DSC analysis, and the results are shown in Figure 1. As shown in Figure 1a, there is an exothermic peak (1st) in the range of 68-104°C, an endothermic peak in the range of 124-155°C, and another exothermic peak (2nd) in the range of 155-205°C for the mixture of FGE and DBMI. The former exothermic peak(1st) is due to the DA polymerization reaction, and the latter exothermic peak(2nd) is self-polymerization of DBMI, while the endothermic peak is due to the reversible DA reaction. There is an exothermic peak between 105°C and 232°C in the DSC curve for the mixture of FGE and ODA, which is due to the ring-opening reaction of oxirane rings with amino groups. For the mixture of ODA and DBMI, there is an endothermic peak between 90°C and 150°C due to the melting of the mixture. Usually, the Michael addition reaction between the diene of DBMI and the amino group of ODA is exothermic and usually occurs above 130°C [29,30]. As shown in the curve of the DBMI and ODA, the exothermic phenomenon occurs above 150°C. As shown in Figure 1b, the thermal curing reaction of FGE-ODA-DBMI resin includes three stages in the range of 40-160°C. The first one (67-102°C) is owing to the DA reaction, and the second one (107-125°C) is due to the ring-opening reaction between oxirane rings and amino groups, and then the third one (125-153°C) is attributed to the r-DA reaction. The reactions between FGE and HBMI, FGE and ODA, HBMI and ODA, and among HBMI, FGE and ODA are investigated by DSC analysis, and the results are shown in Figure S3.

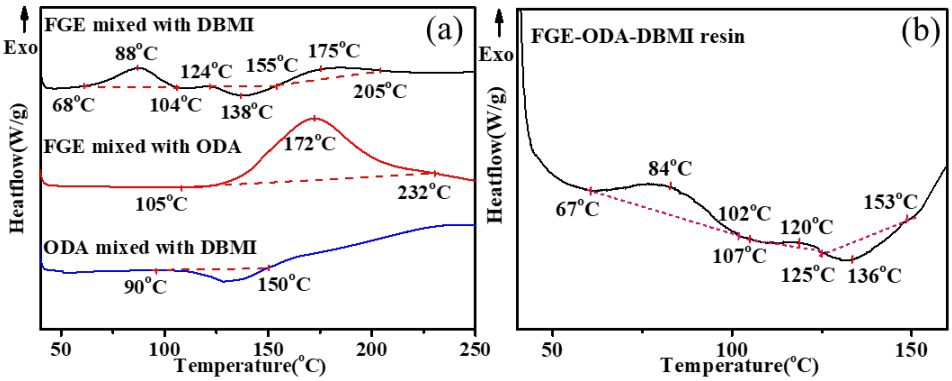

Figure 1. DSC curves of FGE mixed with DBMI, FGE mixed with ODA, ODA mixed with DBMI (a), DSC curves of FGE-ODA-DBMI resin (b).

Three curing procedures, *i.e.*, 90°C /36 h, 110°C /36 h, and 110°C /12 h + 90°C /24 h, for the resins are designed. The FGE-ODA-DBMI resins are cured under three different curing procedures, and the resultant cured resins are noted as cured FGE-ODA-DBMI-1 resin, cured FGE-ODA-DBMI-2 resin and cured FGE-ODA-DBMI-3 resin, respectively. The flexural properties of cured FGE-ODA-DBMI resins are shown in Figure 2a**.** Cured FGE-ODA-DBMI-3 resin has the highest flexural strength (125 MPa) and flexural modulus (4.30 GPa). For cured FGE-ODA-DBMI-1 resin, the ring-opening reaction between oxirane rings and amino groups has not yet taken place at 90°C. Thereby cured FGE-ODA-DBMI-1 resin has the lowest flexural strength. When the resin is heated at 110°C for 36 h, the ring-opening reaction between oxirane rings and amino groups partially occurs while the DA reaction is not obvious during this curing temperature, meaning the resulting resin is further cross-linked. The flexural properties further increase. When the resin is heated at 110°C for 12 h and then at 90°C for another 24 h, the partially cross-linked resin continues to form DA bonds, leading to a higher cross-linking degree, hence cured FGE-ODA-DBMI-3 resin has the highest flexural properties. The effect of three curing procedures on the flexural properties of the cured FGE-ODA-HBMI resin is also investigated, and the results are shown in Figure 2b. Similarly, cured FGE-ODA-HBMI-3 resin possesses the highest flexural properties. Therefore, the curing procedure (110°C /12 h + 90°C /24 h) is

Preprints (www.preprints.org) | NOT PEER-REVIEWED | Posted: 30 June 2023 doi:10.20944/preprints202306.2118.v1

optimal for FGE-ODA-DBMI and FGE-ODA-HBMI resins. The FGE-ODA-BMI resins will be cured with the above optimal curing procedure unless otherwise stated.

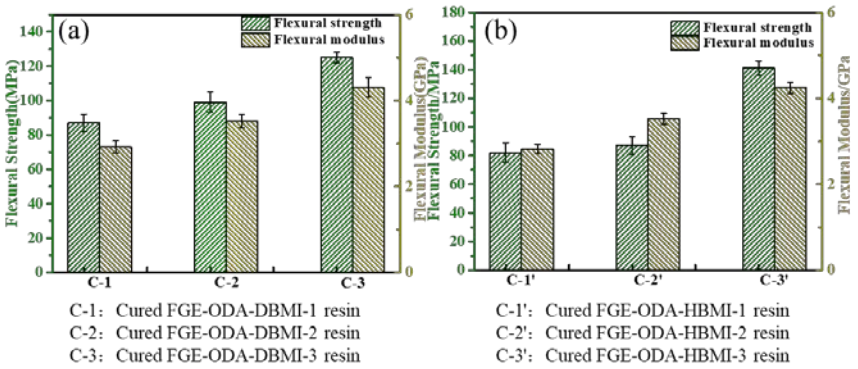

Figure 2. Flexural properties of cured FGE-ODA-BMI resins under three curing procedures: Cured FGE-ODA-DBMI resin (a), cured FGE-ODA-HBMI resin (b).

FT-IR spectroscopy is used to analyze the changes of the characteristic functional groups of the cured FGE-ODA-DBMI resin and its raw material, as shown in Figure 3a. The disappearance of the asymmetrical stretching (918 cm^{-1}) of oxirane rings in the cured FGE-ODA-DBMI resin and the appearance of the extensive absorption at about 3450 cm^{-1} corresponding to hydroxyl groups generated through the ring opening reaction between ODA and FGE reveal that oxirane rings react with amino groups. The peaks at 2930 cm^{-1} and 2860 cm^{-1} are attributed to the antisymmetric and symmetric stretching vibration of $-CH_2$ in turn, and the peak at 1424 cm^{-1} is due to the bending vibration of $-CH_2$. The appearance of a new peak at 1776 cm^{-1} corresponding to succinimide rings generated through DA reaction confirms the successful synthesis of cross-linked networks. The pattern of change for the cured FGE-ODA-HBMI resin is similar and shown in Figure S4a. Meanwhile, FT-IR spectroscopy is used to analyze the changes of the characteristic functional groups of FGE-ODA-DBMI resin during the curing process (Figure 3b). As the curing time of FGE-ODA-DBMI resin increases, the C-O-C stretching vibration peak on the oxirane ring at 1254 cm^{-1} gradually decreases, and the C-N characteristic peak at 1668 cm^{-1} gradually increases. When the resin is cured at 110°C for 12 h, the C-O-C peak disappears, and the C-N peak no longer increases. This result shows that oxirane rings reacts with amino groups. A new peak is identified at 1776 cm^{-1}, which is specific to the DA adduct of maleimide [25]. The absorption peak at 1776 cm^{-1} no longer increases when the curing procedure changes from 110°C /12 h + 90°C/24 h to 110°C /12 h + 90°C/30 h, indicating that the curing procedure (110°C /12 h + 90°C /24 h) for FGE-ODA-DBMI resin is reasonable. The pattern of change for FGE-ODA-HBMI resin is similar and would not be repeated (Figure S4b). A Soxhlet extractor is used to measure the content of soluble components in resins of different structures to determine the curing degree of the resin. The content of soluble components in cured FGE-ODA-DBMI resin and cured FGE-ODA-HBMI resin are 2.21% and 1.29%, respectively. The content of soluble components decreases when the flexible structure is introduced into the resin (FGE-ODA-HBMI), This demonstrates that cured FGE-ODA-HBMI resin possesses the higher cross-linking degree than cured FGE-ODA-DBMI resin.

Preprints (www.preprints.org) | NOT PEER-REVIEWED | Posted: 30 June 2023 doi:10.20944/preprints202306.2118.v1

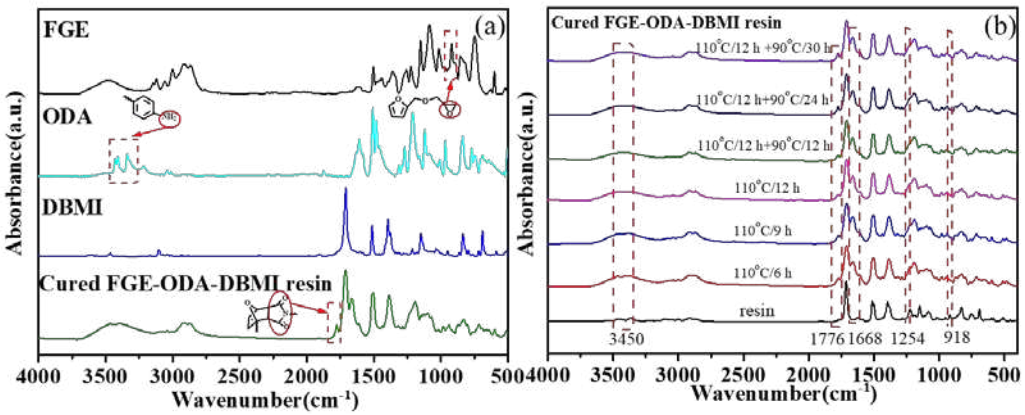

Figure 3. FT-IR spectra of cured FGE-ODA-DBMI resin and its raw materials (a), and FGE-ODA-DBMI resin at different curing stage (b).

3.2. Thermal property of the cured FGE-ODA-BMI resins

Thermoreversibility of the resins is characterized by DSC analysis, and the DSC curves for cured FGE-ODA-BMI resins are shown in Figure 4. As shown in Figure 4a, the reversible Diels-Alder (r-DA) reaction peak temperature of the cured FGE-ODA-HBMI resin (141°C) is higher than that of the cured FGE-ODA-DBMI resin (130°C). This is because the flexible structure in the cured FGE-ODA-HBMI resin gives molecular chains greater mobility. The TGA curves of the resins with different structures are shown in Figure 4b. The decomposition does not happen below 150°C, which further ensures the thermoreversibility. The initial weight loss of resin is because the DA adducts dehydrates to form a benzene ring [31], which is shown in Figure 5. Cured FGE-ODA-DBMI resin dehydrates in the range of 150-300°C with a weight loss of 4.74%, while cured FGE-ODA-HBMI resin dehydrates in the range of 150-320°C with a weight loss of 5.56%. These two results are consistent with the theoretical calculated values of 4.69% and 5.26%, respectively.

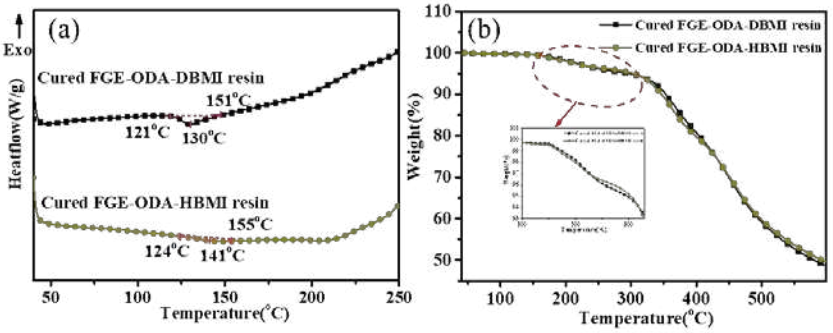

Figure 4. DSC curves of cured FGE-ODA-BMI resins (a), TGA curves of cured FGE-ODA-BMI resin (b).

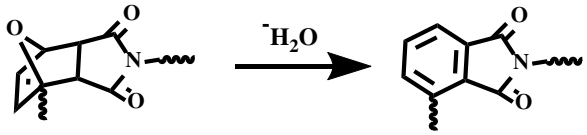

Figure 5. Schematic representation of the dehydrative aromatization of DA adducts.

3.3. Reversible performance of the cured FGE-ODA-BMI resins

The reversibility of the cured FGE-ODA-BMI resin is further analyzed by DSC tests. As shown in Figure 6a, the cured FGM-ODA-DBMI is firstly heated from 20°C to 140°C at a heating rate of 10°C·min^{-1} (*1st heating*), and immediately cooled to 20°C at a cooling rate of 10°C·min^{-1} (*1st cooling*),

Preprints (www.preprints.org) | NOT PEER-REVIEWED | Posted: 30 June 2023 doi:10.20944/preprints202306.2118.v1

and then heated to 140°C again at the same heating rate (*2nd heating*). There is an endothermic peak at 130°C and 131°C in *1st heating* and *2nd heating*, respectively. At the same time, an exothermic peak appears at about 90°C in *1st cooling*. The results indicate that for the cured FGE-ODA-DBMI resin, the DA reaction occurs at about 90°C, and the r-DA reaction does at about 130°C. As shown in Figure 6b, an endothermic peak for the cured FGE-ODA-HBMI resin appears at 142°C and 143°C in *1st heating* and *2nd heating*, respectively. Meanwhile, there is an exothermic peak at about 95°C in *1st cooling*. The results indicate that for the cured FGE-ODA-HBMI resin, the DA reaction occurs at about 95°C, and the r-DA reaction does at about 140°C.

The reversibility of cured FGE-ODA-BMI resins are verified by sol-gel transformation process. The cured FGE-ODA-DBMI resin is taken as an example. The cured FGE-ODA-DBMI resin slightly swell after immersed in DMF at 50°C for 6 h. The phenomenon indicates that the cured FGE-ODA-DBMI resin is cross-linked and thus insoluble in DMF (Figure 7b). Then when heated at 140°C, the resin quickly turned into a reddish-brown liquid (Figure 7c), which indicate that the r-DA reaction of DA bonds in the network have taken place. Due to the reduction in molecular weights, the depolymerized resin is easily dissolved in DMF. Subsequently, when the liquid is heated at 90°C for a period of time, the broken DA bonds reunite to form a cross-linked network. As the DA reaction progresses, the cross-linking degree gradually increases. After 4 h, the resin forms a gel (Figure 7d). Finally, the resin repolymerizes into a reddish-brown lumpy solid. The sol-gel transformation process of the cured FGE-ODA-HBMI resin is similar to that of the cured FGE-ODA-DBMI resin (Figure S5). These results show that the cured FGE-ODA-DBMI resin and the cured FGE-ODA-HBMI resin are thermosetting resins with good thermal reversibility.

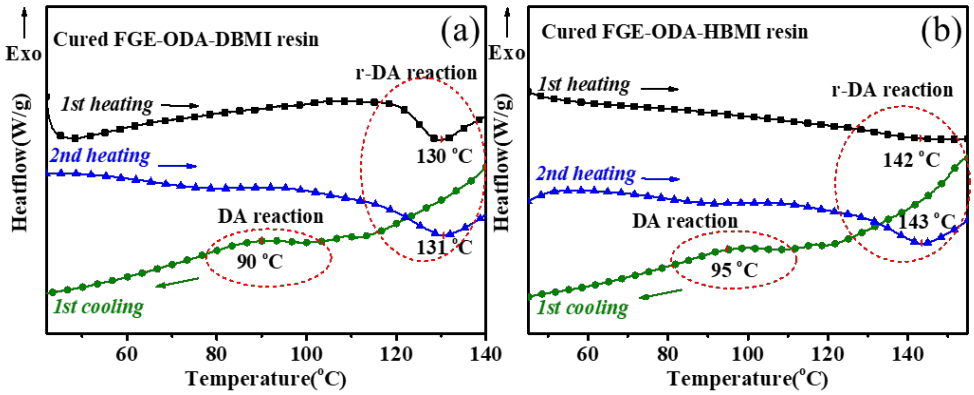

Figure 6. DSC curves of the cured FGE-ODA-DBMI resin (a), and the cured FGE-ODA-HBMI resin (b).

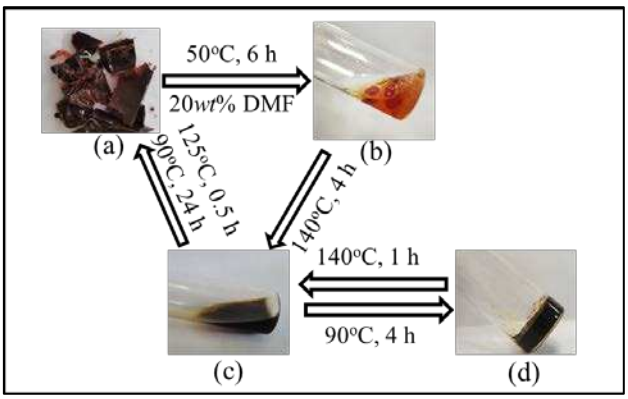

Figure 7. The photos of sol-gel transformation process for the cured FGE-ODA-DBMI resin: the small fragments of cured resin (a), the swelled state of cured resin (b), the dissolved state of cured resin (c), the gel state of cured resin (d).

Preprints (www.preprints.org) | NOT PEER-REVIEWED | Posted: 30 June 2023 doi:10.20944/preprints202306.2118.v1

Since the resin is thermally reversible, the fractured resin could be reshaped by hot-pressing method to form a homogeneous solid. The schematic repair process of the cured FGE-ODA-BMI resins is shown in Figure 8. The repair efficiency of the resin is determined by testing the flexural strength of the resin after hot pressing. As listed in Table 1, cured FGE-ODA-DBMI and FGE-ODA-HBMI resins possess the flexural strength of 125 MPa and 141 MPa, and the flexural moduli of 4.30 GPa and 4.25 GPa respectively, indicating that the flexible structures in the resin could increases flexural strength but slightly reduce flexural modulus. Because cured FGE-ODA-DBMI resin has lower r-DA reaction peak temperature, the r-DA reaction is easier to occur, which is beneficial to repair. Thus, the repair efficiency of cured FGE-ODA-DBMI resin is higher than that of cured FGE-ODA-HBMI resin. In addition, the flexural property of the resin declines after repair. This is because furan rings generated by the depolymerization of DA bonds is easily oxidized at high temperature [32].

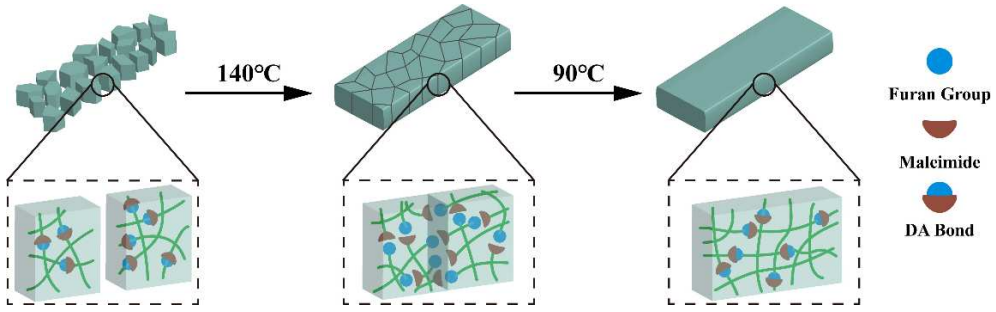

Figure 8. Schematic repair process of the cured FGE-ODA-BMI resins.

After the cured FGE-ODA-BMI resins were reshaped by hot-pressing method, the flexural properties are tested and the retention rate is calculated. The initial resins are named R-0, and the resins reprocessed for the first, twice and third time are named R-1, R-2 and R-3, respectively. As shown in Table 1, after the cured FGE-ODA-DBMI resin is recompressed for three times, the flexural strength is 83 MPa, giving a retention rate of 66.4% compared to the initial flexural strength. Similarly, the cured FGE-ODA-HBMI resin has a retention rate of 61.1% after repressed three times.

Table 1. Changes in flexural properties after multiple processing.

Sample	Cured FGE-ODA-DBMI resin			Cured FGE-ODA-HBMI resin		
	Flexural strength (MPa)	Flexural modulus (GPa)	Rretention rate (%)	Flexural strength (MPa)	Flexural modulus (GPa)	Rretention rate (%)
R-0	125±3	4.30±0.23	-	141±5	4.25±0.13	-
R-1	109±7	4.08±0.15	87.2	111±9	3.95±0.17	78.7
R-2	98±8	3.82±0.23	78.4	102±5	3.87±0.21	72.3
R-3	83±6	3.69±0.19	66.4	86±3	3.68±0.16	61.1

4. Conclusions

In this paper, two kinds of thermally reversible cross-linking resins (FGE-ODA-DBMI, FGE-ODA-HBMI) are prepared by changing the structure of BMI. And the properties of FGE-ODA-DBMI and FGE-ODA-HBMI resins are studied. First, the curing process of the two resins is studied by DSC and FT-IR analyses. The optimal curing process of 110°C /12 h + 90°C /24 h is determined. Secondly, the reversibility of the cured FGE-ODA-DBMI and FGE-ODA-HBMI resins is analyzed by DSC tests. DA reaction occurs at about 90°C and r-DA reaction occurs at about 140°C for FGE-ODA-BMI resins. At the same time, the thermal reversible behavior of resin is verified by the sol-gel transformation process. Finally, the cured resin is reshaped by hot-pressing method to form a homogeneous solid. The cured FGE-ODA-DBMI and FGE-ODA-HBMI resins have a repair efficiency of over 75% at the beginning. After being repressed for three times, both resins retain more than 60% of flexural strength. Compared to FGE-ODA-HBMI resin, FGE-ODA-DBMI resin with a rigid structure has a

lower flexural property but a better reversibility. These results would provide a reference for the design and preparation of high-performance reversible resins.

Supplementary Materials: The following supporting information can be downloaded at the website of this paper posted on Preprints.org. Figure S1: ^{1}H-NMR spectra (a), FT-IR spectra (b), EI-MS spectra (c), and DSC curve (d); Figure S2: ^{1}H-NMR spectra (a), FT-IR spectra (b), EI-MS spectra (c), and DSC curve (d); Figure S3: DSC curves of FGE mixed with HBMI, FGE mixed with ODA, ODA mixed with HBMI (a), DSC curves of FGE-ODA-HBMI resin (b); Figure S4: FT-IR spectra of the cured FGE-ODA-HBMI resin and its raw materials(a), and FGE-ODA-HBMI resin at different curing stage (b); Figure S5: The photos of sol-gel transformation process for the cured FGE-ODA-HBMI resin: the small fragments of cured resin (a), the swelled state of cured resin (b), the dissolved state of cured resin (c), the gel state of cured resin (d).

Author Contributions: Jiawen Wang: writing-original draft, writing-review and editing, methodology, formal analysis, conceptualization, data curation, investigation; **Jixian Li:** formal analysis, visualization; **Jun Zhang:** validation, visualization; **Shuyue Liu:** data curation; **Liqiang Wan:** investigation, methodology, project administration; **Zuozhen Liu:** writing-review and editing: **Farong Huang:** conceptualization, funding acquisition, project administration, resources, supervision, writing-review and editing.

Data Availability Statement: The datasets generated during and/or analyzed during the current study are available from the corresponding author on reasonable request.

Acknowledgments: The authors gratefully acknowledge the support of the National Key R&D Program of China (No. 2022YFB3709201) and the Fundamental Research Funds for the Central Universities (JKD01231701).

Conflicts of Interest: The authors state no conflict of interest.

References

1. Van den Tempel P, Picchioni F, Bose RK. Designing end-of-life recyclable polymers via Diels-Alder chemistry: A review on the kinetics of reversible reactions. Macromol Rapid Commun. 2022;43(13): 2200023. doi:10.1002/marc.202200023.
2. Ma SQ, Webster DC. Degradable thermosets based on labile bonds or linkages: A review. Prog. Polym. Sci. 2018;76: 65-110. doi:10.1016/j.progpolymsci.2017.07.008.
3. Zou WK, Dong JT, Luo YW, Zhao Q, Xie T. Dynamic covalent polymer networks: from old chemistry to modern day innovations. Adv. Mater. 2017;29 (14): 1606100. doi:10.1002/adma.201606100.
4. Amamoto Y, Kamada J, Otsuka H, Takahara A, Matyjaszewski K. Repeatable photoinduced self-healing of covalently cross-linked polymers through reshuffling of trithiocarbonate units. Angew. Chem. Int. Ed. 2011;123 (7): 1698-1701. doi:10.1002/anie.201003888.
5. Yoon JA, Kamada J, Koynov K, Mohin J, Nicolaÿ R, Zhang YZ, et al. Self-healing polymer films based on thiol-disulfide exchange reactions and self-healing kinetics measured using atomic force microscopy. Macromolecules. 2011;45 (1): 142-149. doi:10.1021/ma2015134.
6. Montarnal D, Capelot M, Tournihac F, Leibler L. Silica-like malleable materials from permanent organic networks. Science. 2011;334 (6058): 965-968. doi:10.1126/science.1212648.
7. Demongeot A, Mougnier J, Okada S, Soulié-Ziakovic C, Tournilhac F. Coordination and catalysis of Zn^{2+} in epoxy-based vitrimers. Polym. Chem. 2016;7 (27): 4486-4493. doi:10.1039/c6py00752j.
8. Denissen W, Rivero G, Nicolaÿ R, Leibler L, Winne JM, Du Prez FE. Vinylogous urethane vitrimers. Adv. Funct. Mater. 2015;25 (16): 2451-2457. doi:10.1002/adfm.201404553.
9. Taynton P, Yu K, Shoemaker RK, Jin YH, Qi HJ, Zhang W. Heat- or water-driven malleability in a highly recyclable covalent network polymer. Adv. Mater. 2014;26 (23): 3938-3942. doi:10.1002/adma.201400317.
10. Lei XF, Jin YH, Sun HL, Zhang W. Rehealable imide-imine hybrid polymers with full recyclability. J. Mater. Chem. A. 2017;5 (40): 21140-21145. doi:10.1039/c7ta07076d.
11. Zheng PW, McCarthy TJ. A surprise from 1954: siloxane equilibration is a simple, robust, and obvious polymer self-healing mechanism. JACS. 2012;134 (4): 2024-2027. doi:10.1021/ja2113257.
12. Obadia M, Mudraboyina BP, Serghei A, Montarnal D, Drockenmuller E. Reprocessing and recycling of highly cross-linked ion-conducting networks through transalkylation exchanges of C-N bonds. JACS. 2015;137 (18): 6078-6083. doi: 10.1021/jacs.5b02653.
13. Lu YX, Tournilhac F, Leibler K, Guan ZB. Making insoluble polymer networks malleable via olefin metathesis. JACS. 2012;134 (20): 8424-8427. doi:10.1021/ja303356z.
14. Goodman SH, Dodiuk H. Handbook of thermoset plastics. William Andrew; 2014.
15. Liu YL, Chuo TW. Self-healing polymers based on thermally reversible Diels-Alder chemistry. Polym. Chem. 2013;4 (7): 2194-2205. doi:10.1039/c2py20957h.

16. Min YQ, Huang SY, Wang YX, Zhang ZJ, Du BY, Zhang XH, et al. Sonochemical transformation of epoxy-amine thermoset into soluble and reusable polymers. Macromolecules. 2015;48 (2): 316-322. doi: 10.1021/ma501934p.
17. Gandini A, Lacerda TM. Furan polymers: State of the art and perspectives. Macromol. Mater. Eng. 2022;307(6): 2100902. doi:10.1002/mame.202100902.
18. Yang TC, Yeh CH. Morphology and mechanical properties of 3D printed wood fiber/polylactic acid composite parts using fused deposition modeling (FDM): The effects of printing speed. Polymers-Basel. 2020;12 (6): 1334. doi:10.3390/polym12061334.
19. Navarro-Baena I, Sessini V, Dominici F, Torre L, Kenny JM, Peponi L. Design of biodegradable blends based on PLA and PCL: From morphological, thermal and mechanical studies to shape memory behavior. Polym. Degrad. Stab. 2016;132: 97-108. doi:10.1016/j.polymdegradstab.2016.03.037.
20. Pauloehrl T, Delaittre G, Winkler V, Welle A, Bruns M, Bçrner HG, et al. Adding spatial control to click chemistry: phototriggered Diels-Alder surface (bio)functionalization at ambient temperature. Angew. Chem. Int. Ed. 2012;51(4): 1071-1074. doi:10.1002/anie.201107095.
21. Fan MJ, Liu JL, Li XY, Zhang JY, Cheng J. Recyclable Diels-Alder furan/maleimide polymer networks with shape memory effect. Ind. Eng. Chem. Res. 2014;53(42): 16156-16163. doi:10.1021/ie5028183.
22. Yasuda K, Takahashi Y, Sugane K, Shibata M. Self-healing high-performance thermosets utilizing furan/maleimide Diels-Alder, epoxy/amine nucleophilic ring-opening, and maleimide/amine michael reactions. Polym. Bull. 2021;79 (10): 8455-8469. doi:10.1007/s00289-021-03912-6.
23. Shabani P, Shokrieh MM, Zibaei I. Effect of the conversion degree and multiple healing on the healing efficiency of a thermally reversible self-healing polymer. Polym. Adv. Technol. 2019;30(11): 2906-2917. doi:10.1002/pat.4723.
24. Abdollahi H, Salimi A, Barikani M, Samadi A, Rad S, Zanjanijam AR. Systematic investigation of mechanical properties and fracture toughness of epoxy networks: Role of the polyetheramine structural parameters. J. Appl. Polym. Sci. 2018;136 (9): 47121. doi:10.1002/app.47121.
25. Ma MM, Wang XY, Yu ZE, Wan LQ, Huang FR. High impact polytriazole resins for advanced composites. Des. Monomers Polym. 2020;23 (1): 50-58. doi:10.1080/15685551.2020.1761584.
26. Dhanaraju G, Golla S, Ben BS, Vikram KA. Interfacial and matrix healing of thermally reversible bismaleimide infused Graphene Nano Platelets reinforced polymer nanocomposite through Diels-Alder bonding. Mater. Today Commun. 2022;31: 103753. doi.org/10.1016/j.mtcomm.2022.103753.
27. Polgar LM, Cerpentier RRJ, Vermeij GH, Picchioni F, van Duin M. Influence of the chemical structure of cross-linking agents on properties of thermally reversible networks. Pure Appl. Chem. 2016;88 (12): 1103-1116. doi:10.1515/pac-2016-0804.
28. Lorero I, Rodríguez A, Campo M, Prolongo SG. Thermally remendable, weldable, and recyclable epoxy network crosslinked with reversible Diels-alder bonds. Polymer 2022;259: 125334. doi.org/10.1016/j.polymer.2022.125334.
29. Li JH, Zhang GP, Deng LB, Jiang K, Zhao SF, Gao YJ, et al. Thermally reversible and self-healing novolac epoxy resins based on Diels-Alder chemistry. J. Appl. Polym. Sci. 2015;132 (26): 42167. doi:10.1002/app.42167.
30. Zolghadr M, Shakeri A, Zohuriaan-Mehr MJ, Salimi A. Self-healing semi-IPN materials from epoxy resin by solvent-free furan-maleimide Diels-Alder polymerization. J. Appl. Polym. Sci. 2019;136 (40): 48015. doi: 10.1002/app.48015.
31. Settle AE, Berstis L, Rorrer NA, Roman-Leshkóv Y, Beckham GT, Richards RM, et al. Heterogeneous Diels-Alder catalysis for biomass-derived aromatic compounds. Green Chem. 2017;19 (15): 3468-3492. doi:10.1039/C7GC00992E.
32. Canary SA, Stevens PM. Thermally reversible crosslinking of polystyrene via the furan-maleimide Diels-Alder reaction. J. Polym. Sci., Part A: Polym. Chem. 1992;30: 1755-1760. doi:10.1002/pola.1992.080300829.